engineering proceedings

MDPI

Proceeding Paper

Position and Speed Tracking of DC Motor Based on Experimental Analysis in LabVIEW †

Muhammad Ilyas [1,*], Attaullah Khidrani [2] and Syed Ali Raza Shah [3]

1 Department of Biomedical Engineering, Balochistan University of Engineering and Technology Khuzdar, Khuzdar 98100, Balochistan, Pakistan
2 Department of Electrical Engineering, Balochistan University of Engineering and Technology Khuzdar, Khuzdar 98100, Balochistan, Pakistan; khidraniatta@buetk.edu.pk
3 Department of Mechanical Engineering, Balochistan University of Engineering and Technology Khuzdar, Khuzdar 98100, Balochistan, Pakistan; razadopasi@buetk.edu.pk
* Correspondence: m.ilyas@buetk.edu.pk
† Presented at the 8th International Electrical Engineering Conference, Karachi, Pakistan, 25–26 August 2023.

Abstract: DC motors are widely used in industries to provide mechanical power in speed and torque. The position and speed control of DC motors is receiving interest from the scientific community in robotics, especially in robotic arms, a flexible joint manipulator. The current research work is based on the position control of DC motors using experimental investigations in LabVIEW. The linear control strategy is applied to track the position and speed of the DC motor with comparative analysis in the LabVIEW platform and simulation analysis in MATLAB. The tracking error in the hardware setup based on LabVIEW programming is slightly greater than the simulation analysis in MATLAB due to the inertial load of the motor during steady-state conditions. The controller output shows the input voltage applied to the DC motor varies between 0 and 8 V to ensure minimal steady error while tracking the position and speed of the DC motor.

Keywords: DC motor; LabVIEW; proportional integral derivative control; position tracking

check for updates

Citation: Ilyas, M.; Khidrani, A.; Shah, S.A.R. Position and Speed Tracking of DC Motor Based on Experimental Analysis in LabVIEW. *Eng. Proc.* **2023**, *46*, 4. https://doi.org/10.3390/engproc2023046004

Academic Editors: Abdul Ghani Abro and Saad Ahmed Qazi

Published: 20 September 2023

1. Introduction

In the current technological era, the design and development of high-performance motor drives is increasing exponentially due to their applications in electric trains, robotics, DC appliances, biomedical equipment and other industrial applications. Generally, the high-performance motor drive system is based on proficient speed command tracking and a load regulating system to perform any task in industry [1–3]. DC drives are normally less expensive and provide excellent control of speed for acceleration and deceleration compared to AC motors. The most common emerging applications of DC motors are robotic and electrical equipment. Therefore, the speed and position control of DC motors has been investigated in the last few decades. One challenging aspect of the DC motor when designing a control system is the uncertain and nonlinear characteristic which degrades the performance of controllers [4,5]. In addition to industrial applications, DC motors are extensively used in various serve devices like flight simulators, optoelectronic tracking platforms and missile electromechanical actuators. However, various uncertainties exist in motor serve systems including modeling errors, torque disturbances and parametric perturbations hindering its performance and efficacy [6–8]. The disturbance torques can be quite large for cheap DC motors and can cause performance issues. The conventional proportional integral derivative (PID) controller may not be very effective for eliminating the speed ripples of motors with small inertia due to the periodic nature of the disturbance torque [9–13].

The robust control method based on the disturbance observer shows a strong inhibitory effect against various external disturbances and parametric variations by improving the control performance of the system. The high-precision serve system relies on such robust control strategies. The sliding mode control variable structure control (SMVSC) is a nonlinear control strategy exhibiting strong robustness against external disturbances and parametric variations [14–20]. Besides this, the global sliding mode control reflects the system trajectory on the sliding surface by constructing nonlinear switching function and later eliminates the initial reaching function [21–23]. The current research is based on the position and speed control of the DC motor for undergraduate students to investigate and compare the performance of DC motors using hardware setups based on LabVIEW programming and simulation analysis in MATLAB. The mathematical model of the DC motor is derived using physics and electromagnetism laws. The PID controller is designed to track the position of the DC motor. The performance of the PID controller is investigated while tracking the position and speed during steady-state conditions. It is observed that when using hardware based on experimental setup, the tracking error is slightly greater compared to the simulation analysis in MATLAB due to the inertial load of the DC motor during the switching phase of the pulse generator signal. The controller gains and specification of the input reference signal are the same for both analyses. The rest of the paper is organized as follows: Section 2 describes the mathematical model DC motor; Section 3 works on the control scheme design using a PID controller; Section 4 discusses the simulation results in MATLB and the hardware implementation results in LabVIEW; Section 5 provides the conclusions.

2. Mathematical Model of DC Motor

The DC motor is an electromechanical device that provides displacement at the output side for various voltage levels at the input. The mathematical model of an armature-controlled DC motor was derived by Mablekos in 1980. Figure 1 shows the permanent magnets that generate the magnetic field referred to as the fixed field. The armature is a rotating part through the current; $i_A(t)$ is the flow, and the experienced force at $90°$ can be stated as $F = ILB\sin\theta$ for $\theta = 90°$, $F = ILB$, while L is the length of the conductor, and B is the magnetic field strength. The resulting torque occurs due to the force experienced by the armature, which causes the armature to rotate. The $e_{indcued} = vBL$, v is the velocity of the conductor, $e_{indcued}$ is the induced voltage that is proportional to the angular speed of the armature in the magnetic field. The induced voltage can be stated as $V_b = K_b \frac{d\theta_m(t)}{dt} = K_b s\theta_m(s)$. Applying KVL to the closed-loop circuit is shown in Figure 1 as

$$E(t) = i_a(t)R_a + L_a \frac{di_a}{dt} + V_b(t) \quad (1)$$

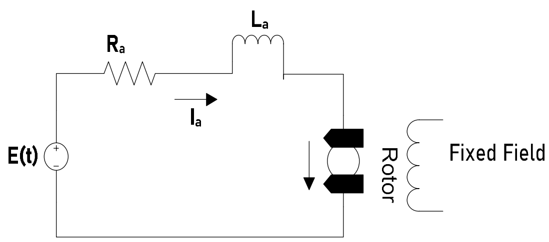

Figure 1. Electrical circuit of DC motor.

Applying the Laplace transform to Equation (1) as in Equation (2),

$$E(s) = I_a(s)(R_a + L_a s I_a(s) + V_b(s) \quad (2)$$

Putting the value of $V_b = K_b \frac{d\theta_m(t)}{dt} = K_b s\theta_m(s)$ in Equation (2) as in Equation (3),

$$E(s) = I_a(s)(R_a + L_a s) + K_b s\theta_m(s) \quad (3)$$

The torque $\mathrm{T_m(s)}$ developed by the motor is proportional to the armature current $I_a(s)$, which can be expressed as $\mathrm{T_m(s)} = \mathrm{K_t} I_a(s)$ or $I_a(s) = \frac{\mathrm{T_m(s)}}{\mathrm{K_t}}$. Then, the value of $I_a(s)$ is put in Equation (3) as in Equation (4):

$$E(s) = \frac{\mathrm{T_m(s)}}{\mathrm{K_t}}(R_a + L_a s) + K_b s \theta_m(s) \tag{4}$$

Expressing the torque in terms of $\theta_m(s)$, J_m is the moment of inertia of the armature J_a and load inertia for J_{load} for the QENT DC motor $J_m = J_a + J_{load}$. This can be expressed as $\mathrm{T_m(s)} = (\mathrm{J_m s^2} + \mathrm{D_m s})\theta_m(s)$ and its value is incorporated into Equation (4) as in Equation (5):

$$E(s) = \frac{(\mathrm{J_m s^2} + \mathrm{D_m s})\theta_m(s)}{\mathrm{K_t}}(R_a + L_a s) + K_b s \theta_m(s) \tag{5}$$

Assuming that the armature $R_a >> L_a$ as L_a can be neglected in Equation (5) as in Equation (6),

$$E(s) = \frac{(\mathrm{J_m s^2} + \mathrm{D_m s})\theta_m(s)}{\mathrm{K_t}} \times R_a + K_b s \theta_m(s) \tag{6}$$

Simplifying Equation (6) as in Equation (7),

$$\frac{\theta_m(s)}{E(s)} = \frac{K_t/R_a}{s(J_m s + \frac{K_t K_b}{R_a})} \tag{7}$$

The physical parameters of DC motor is shown in Table 1 with their description and unit values.

Table 1. Physical parameter of the DC motor.

Parameter Name	Description	Unit
R_a	Terminal resistance	8.4 Ω
K_t	Torque constant	0.042 Nm/A
K_b	Motor back-emf constant	0.042 V/(rad/s)
J_m	Rotor inertia	4.0×10^{-6} kg m^2
J_l	Load inertia	0.6×10^{-6} kg m^2
L_m	Rotor inductance	1.16 mH
m_l	Estimated damping of the pivot	0.016 kg
m_d	Disk mass	0.053 kg

3. PID Controller Design for Position Tracking of DC Motor

Figure 2 shows the cascaded control strategy based on a PID system to reflect the θ_m to θ_{ref} in a closed-loop scheme.

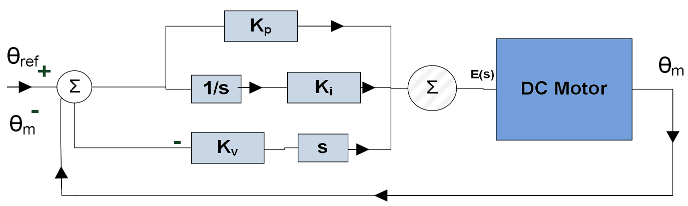

Figure 2. Position control of the DC motor based on a PID controller.

The controller input based on a PID controller can be defined as in Equation (8) [24,25].

$$E(s) = k_p(\theta_{ref} - \theta_m(t)) + k_i \int (\theta_{ref} - \theta_m(t))dt + k_v \frac{d}{dt}(\theta_{ref} - \theta_m(t)) \tag{8}$$

Simplifying and taking the Laplace transform $\mathcal{L}$ of Equation (8) as in Equation (9),

$$E(s) = k_p\theta_{ref}(s) - k_p\theta_m(s) + \frac{k_i}{s}\theta_{ref}(s) - \frac{k_i}{s}\theta_m(s) - k_v s\theta_m(s) \quad (9)$$

By substituting the value of $E(s)$ as the input to the plant from Equation (9) in Equation (10),

$$\frac{\theta_m(s)}{1086.96}\left(s^2 + 45.65s\right) = k_p\theta_{ref}(s) - k_p\theta_m(s) + \frac{k_i}{s}\theta_{ref}(s) - \frac{k_i}{s}\theta_m(s) - k_v s\theta_m(s) \quad (10)$$

Simplifying and rearranging Equation (10) as in Equation (11),

$$\frac{\theta_m(s)}{\theta_{ref}} = \frac{1086.96(k_p s + k_i)}{s^3 + s^2(45.65 + 1086.96k_v) + 1086.96k_p s + 1086.96k_i} \quad (11)$$

The third-order characteristic polynomial equation can be defined as in Equation (12).

$$(s^2 + 2\zeta\omega_n s + \omega_n^2)(s + p_o) = s^3 + (2\zeta\omega_n + p_o)s^2 + (\omega_n^2 + 2\zeta\omega_n p_o)s + \omega_n^2 p_o \quad (12)$$

Then, compare the denominator of Equations (11) and (12) to compute the k_p, k_i and k_v gains of the PID controller for $\zeta = 1$ and $\omega_n = 30$ rad/sec and $p_o = 1$ as $0.883\frac{A}{deg}$, $0.0132\frac{deg}{s}$ and $0.827\frac{A}{\frac{deg}{s}}$, respectively.

4. Simulations and Experimental Hardware Results in MATLAB and LabVIEW

The investigated results achieved based on the simulation results in MATLAB and the experimental analysis using LabVIEW are identified in Section 4. Figure 3a shows the position control of the DC motor based on a PID controller while using the gains values k_p, k_v and k_i shown in Equation (12). The actual position $\theta_m(s)$ accurately tracks the θ_{ref} with a tracking error of less than 5% in the MATLAB simulations. The input to the DC motor is shown in Figure 3b as the input voltage level $E(s)$ that varies from −4 V to 4 V. Figure 3a,b shows that, as the position of the DC motor is varies, the input voltage level also varies between two peaks. The Figure 3a shows that tracking error is quite negligible using MATLAB simulation based on PID controller.

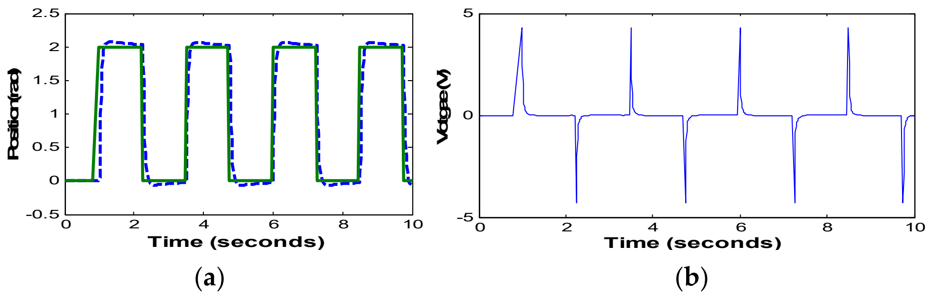

Figure 3. (**a**) Position control of the DC motor in MATLAB; (**b**) controller input voltage level.

Figure 4a shows the position control of the DC motor based on the hardware platform using LabVIEW. The $\theta_m(s)$ shows the measured position of the DC motor tracking the θ_{ref} with a significant steady-state error due to the inertial load of the motor during the switching of the pulse generator signal as a reference position level. Figure 4b shows that the controller output $E(s)$ is voltage applied as the input to the DC motor. The controller output $E(s)$ varies from −4 V to 4 V as the position of the DC motor changes.

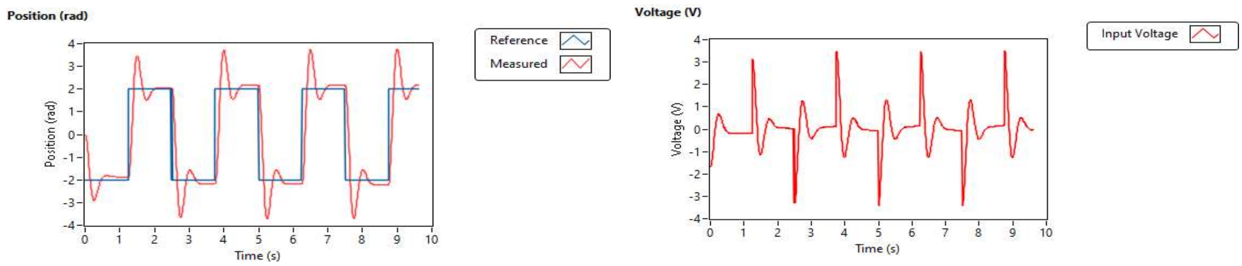

(**a**) (**b**)

Figure 4. (**a**) Position control of the DC motor with the experimental setup using LabVIEW; (**b**) controller output voltage as the input to the DC motor.

Figure 5a shows the speed control of the DC motor based on a PID controller. The ω_m is the actual speed of the DC motor as it tracks the ω_{ref} with minor deviations in tracking error during the switching of the square wave or pulse generator signal. Figure 5b shows the input voltage level being provided to the DC motor as the controller output signal. The amplitude of the input voltage $E(s)$ to the DC motor has a variation of $(0 - 8)$ V.

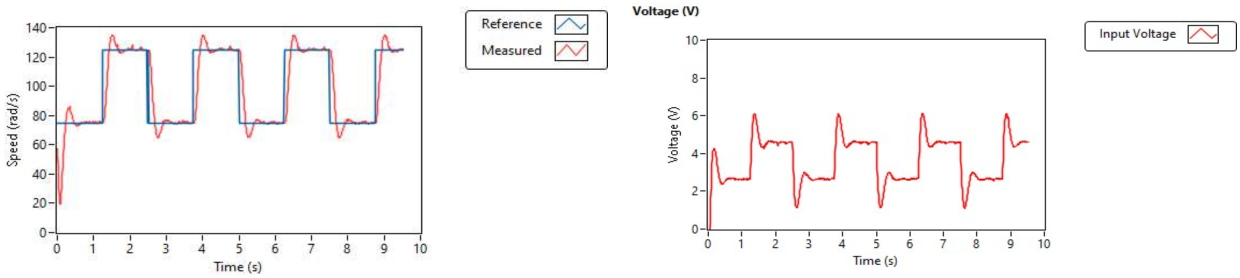

(**a**) (**b**)

Figure 5. (**a**) Speed control of the DC motor based on a PID controller; (**b**) controller output voltage as the input to the DC motor.

5. Conclusions

This paper investigated the position and speed control of the DC motor based on the PID controller and achieved a nominal performance with a steady-state error of less than 5% in a simulation based on MATLAB and experimental analysis using the LabVIEW platform. It is observed that the inertial load impacts the tracking performance of the linear controllers. The speed control of the DC motor has an eminent flexible joint manipulator that can be further extended while handling various perturbations including torque disturbances as well.

Author Contributions: Conceptualization, A.K. and M.I.; methodology, M.I.; software, M.I.; validation, S.A.R.S. and M.I.; formal analysis, A.K.; investigation, M.I.; writing—original draft preparation, M.I.; writing—review and editing, A.K.; supervision, S.A.R.S. All authors have read and agreed to the published version of the manuscript.

Funding: This research received no external funding.

Institutional Review Board Statement: Not applicable.

Informed Consent Statement: Not applicable.

Data Availability Statement: Not applicable.

Conflicts of Interest: The authors declare no conflict of interest.

References

1. Steinbuch, M.; Merry, R.J.; Boerlage, M.L.; Ronde, M.J.; van de Molengraft, M.J. Advanced motion control design. In *The Control Handbook, Control System Applications*, 2nd ed.; CRC Press: Boca Raton, FL, USA, 2010; pp. 1–27.

2. Garpinger, O.; Hägglund, T.; Åström, K.J. Performance and robustness trade-offs in PID control. *J. Process Control* **2014**, *24*, 568–577. [CrossRef]
3. Wang, X.-K.; Sun, Z.-L.; Wang, L.; Feng, D.-Q. Design and research based on fuzzy PID-parameters self-tuning controller with MATLAB. In Proceedings of the 2008 International Conference on Advanced Computer Theory and Engineering, Phuket, Thailand, 20–22 December 2008; pp. 996–999.
4. Wu, Y.; Li, Y.; Zhang, W. A discrete-time chattering free sliding mode control with multirate sampling method for flight simulator. *Math. Probl. Eng.* **2013**, *2013*, 865493. [CrossRef]
5. Ren, Y.; Liu, Z.; Liu, X.; Zhang, Y. A chattering free discrete-time global sliding mode controller for optoelectronic tracking system. *Mathematical Problems in Engineering* **2013**, *2013*, 951492. [CrossRef]
6. Liu, X.; Wu, Y.; Deng, Y.; Xiao, S. A global sliding mode controller for missile electromechanical actuator servo system. *Proc. Inst. Mech. Eng. Part G J. Aerosp. Eng.* **2014**, *228*, 1095–1104. [CrossRef]
7. Juhász, L.; Maas, J. Control of hybrid nanopositioning systems for trajectory-tracking applications. *Mechatronics* **2013**, *23*, 617–629. [CrossRef]
8. Zhang, A.; She, J.; Lai, X.; Wu, M.; Qiu, J.; Chen, X. Robust tracking control of robot manipulators using only joint position measurements. *Math. Probl. Eng.* **2013**, *2013*, 719474. [CrossRef]
9. Pantonial, R.; Kilantang, A.; Buenaobra, B. Performance of a real time disturbance observer in rotational motion electro-mechanical system from stimulated physical actuation. In Proceedings of the TENCON 2012 IEEE Region 10 Conference, Cebu, Philippines, 19–22 November 2012; pp. 1–6.
10. Salameh, J.P.; Sébastien, C.; Etien, E.; Sakout, A.; Rambault, L. Wind profile disturbance isolation and attenuation through an UIO–LPV approach in PMSG-based wind turbines. *IET Control. Theory Appl.* **2020**, *14*, 2924–2936. [CrossRef]
11. Abdulameer, A.; Sulaiman, M.; Aras, M.S.M.; Saleem, D. Tuning methods of PID controller for DC motor speed control. *Indones. J. Electr. Eng. Comput. Sci.* **2016**, *3*, 343–349. [CrossRef]
12. Kong, L.; He, W.; Yang, C.; Li, Z.; Sun, C. Adaptive fuzzy control for coordinated multiple robots with constraint using impedance learning. *IEEE Trans. Cybern.* **2019**, *49*, 3052–3063. [CrossRef] [PubMed]
13. Dursun, E.H.; Durdu, A. Speed control of a DC motor with variable load using sliding mode control. *Int. J. Comput. Electr. Eng.* **2016**, *8*, 219. [CrossRef]
14. Cui, G.; Yu, J.; Shi, P. Observer-based finite-time adaptive fuzzy control with prescribed performance for nonstrict-feedback nonlinear systems. *IEEE Trans. Fuzzy Syst.* **2020**, *30*, 767–778. [CrossRef]
15. Ravikumar, D.; Srinivasan, G.K. Implementation of higher order sliding mode control of DC–DC Buck converter fed permanent magnet DC motor with improved performance. *Automatika* **2023**, *64*, 162–177. [CrossRef]
16. Feng, Y.; Yu, X.; Han, F. High-order terminal sliding-mode observer for parameter estimation of a permanent-magnet synchronous motor. *IEEE Trans. Ind. Electron.* **2012**, *60*, 4272–4280. [CrossRef]
17. Chotai, J.; Narwekar, K. Modelling and position control of brushed DC motor. In Proceedings of the 2017 International Conference on Advances in Computing, Communication and Control (ICAC3), Mumbai, India, 1–2 December 2017; pp. 1–5.
18. Kiruthika, A.; Rajan, A.A.; Rajalakshmi, P. Mathematical modelling and speed control of a sensored brushless DC motor using intelligent controller. In Proceedings of the 2013 IEEE International Conference on Emerging Trends in Computing, Communication and Nanotechnology (ICECCN), Tirunelveli, India, 25–26 March 2013; pp. 211–216.
19. Hameed, H.S. Brushless DC motor controller design using MATLAB applications. In Proceedings of the 2018 1st International Scientific Conference of Engineering Sciences-3rd Scientific Conference of Engineering Science (ISCES), Diyala, Iraq, 10–11 January 2018; pp. 44–49.
20. Dani, S.; Sonawane, D.; Ingole, D.; Patil, S. Performance evaluation of PID, LQR and MPC for DC motor speed control. In Proceedings of the 2017 2nd International Conference for Convergence in Technology (I2CT), Mumbai, India, 7–9 April 2017; pp. 348–354.
21. Jaffery, M.; Aslam, S.; Ghauri, M.; Khuram, M.S.; Rafiq, S.; Khan, S. Real-time implementation of model predictive control on a 16-bit microcontroller for speed control of a DC motor. *J. Eng. Technol.* **2018**, *6*, 415–434.
22. Okoro, I.S.; Enwerem, C. Performance assessment of a model-based DC motor scheme. *Appl. Model. Simul.* **2019**, *3*, 145–153.
23. Adel, Z.; Hamou, A.A.; Abdellatif, S. Design of Real-time PID tracking controller using Arduino Mega 2560for a permanent magnet DC motor under real disturbances. In Proceedings of the 2018 International Conference on Electrical Sciences and Technologies in Maghreb (CISTEM), Algiers, Algeria, 28–31 October 2018; pp. 1–5.
24. Somefun, O.; Akingbade, K.; Dahunsi, F. Speed Control of DC Motors: Optimal Closed PID-Loop Model Predictive Control. *Univers. J. Control Autom.* **2020**, *8*, 9–21. [CrossRef]
25. Niembro-Ceceña, J.A.; Gómez-Loenzo, R.A.; Rodríguez-Reséndiz, J.; Rodríguez-Abreo, O.; Odry, Á. Auto-Regression Model-Based Off-Line PID Controller Tuning: An Adaptive Strategy for DC Motor Control. *Micromachines* **2022**, *13*, 1264. [CrossRef] [PubMed]